Chem Soc Rev

This article was published as part of the

2008 Chemistry at Surfaces issue

Reviewing the latest developments in surface science

All authors contributed to this issue in honour of the 2007 Nobel Prize winner Professor Gerhard Ertl

Please take a look at the issue 10 table of contents to access the other reviews

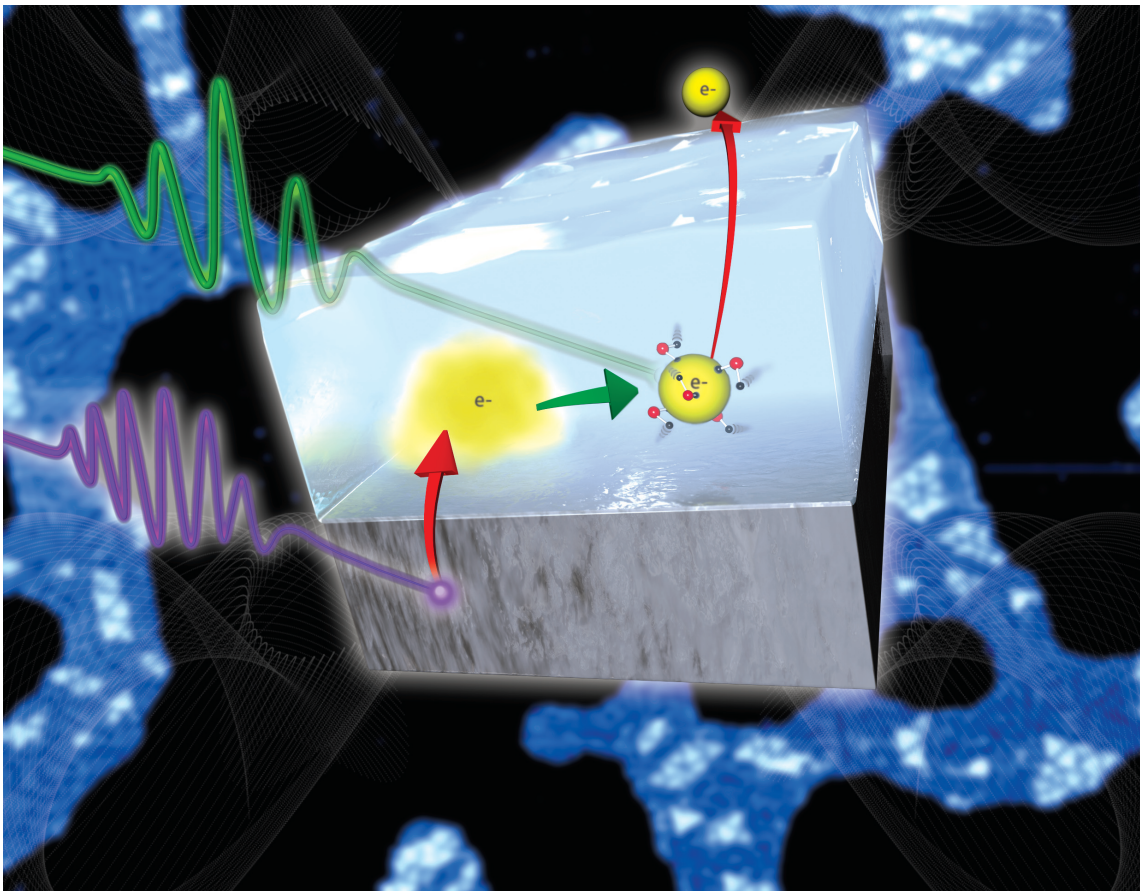

The local structure of molecular reaction intermediates at surfaces†

D. P. Woodruff

Received 22nd May 2008
First published as an Advance Article on the web 4th August 2008
DOI: 10.1039/b719541a

A *critical review* is presented of the results of (experimental) quantitative structural studies of molecular reaction intermediates at surfaces; *i.e.* molecular species that do not exist naturally in the gas phase and, in most cases, are implicated in surface catalytic processes. A brief review of the main experimental methods that have contributed to this area is followed by a summary of the main results. Investigated species include: carboxylates, RCOO– (particularly formate, but also deprotonated amino acids); methoxy, CH_3O–; carbonate, CO_3; ethylidyne, CH_3C–; NH_x and SO_x species; cyanide, CN. As far as possible in the limited range of systems studied, a few general trends are identified (108 references).

1. Introduction

In traditional studies of heterogeneous catalysis it is common to see references to 'the active site', the implication being that a particular local geometry on a surface is where a rate-limiting step in the chemistry occurs, and it is certainly true that many (though not all) such catalytic processes are 'structure sensitive'. An attempt to identify these special sites is certainly one of the motivating factors in quantitative and qualitative studies of surface structure, although other structural phenomena, such as adsorbate-induced surface reconstruction, may play a crucial role in determining catalytic activity but are not necessarily site-specific. A particular challenge in quantitative structural studies of surfaces is to determine the local geometry of reaction intermediates on the surface. These are species that play a key role in the overall reaction, but are present only on the surface and not in the reactant or product gases. Of course, within this definition one might include atomic species that are only present in the gas phase in molecular form. For example, in CO oxidation from a CO–O_2 gas mixture, the atomic O on the catalyst surface arising from dissociative adsorption of the O_2 is surely a key ingredient in the reaction. In general, however, the term is more commonly applied to molecular species, and it is this type of reaction intermediate that forms the subject of this review.

Under reaction conditions, such species may be very short-lived and may also, in some cases, have a low steady-state concentration. 'Reaction conditions' commonly imply 'elevated' pressures: *i.e.* far from ultra-high vacuum (UHV) conditions. While it may be possible to identify reaction intermediates under these conditions by optical methods, most typically infrared absorption spectroscopy, there have so far been no experiments aimed at quantifying the local adsorption geometry of surface reaction intermediates under such conditions. Indeed, even the use of such vibrational spectroscopy to identify the adsorption site of an extremely well-characterised adsorbate species, molecular CO, has been shown to be susceptible to error,[1] and these methods certainly provide no information on chemisorption bondlengths. Instead, quantitative surface structural studies have been performed under static UHV conditions, the adsorbed species being stabilised on the surface by the use of surface temperatures well below those of the steady-state reaction.

While this review is mainly concerned with the *results* of structure determination, some comments on the actual methods that have been used are appropriate, as the relative strengths and weaknesses of different methods need to be borne in mind in assessing the results. Here we should stress that this review is concerned only with *quantitative* methods capable of identifying adsorption sites and bondlengths, and not the more indirect structural assignments that may be inferred from spectroscopic methods or from scanning tunnelling microscopy (STM). We also focus on experimental structure determination; the success of modern density functional theory (DFT) computer codes, combined with the huge increase in low-cost computing power in the past few years has led to very many structure 'determinations' being published, based simply on calculated minimum energy structures. In some cases, such calculations are combined with the use of qualitative experimental techniques (such as STM), greatly

Physics Department, University of Warwick, Coventry, UK CV4 7AL. E-mail: d.p.woodruff@warwick.ac.uk
† Part of a thematic issue covering reactions at surfaces in honour of the 2007 Nobel Prize winner Professor Gerhard Ertl.

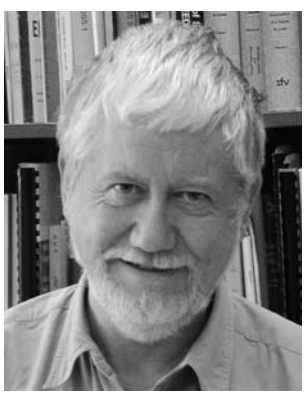

Phil Woodruff

Phil Woodruff is Professor of Physics at the University of Warwick and also has a visiting position at the Fritz Haber Institute in Berlin. He is interested in the development and application of methods to investigate the structural, electronic and chemical properties of surfaces, with a special emphasis on quantitative structure determination, particularly using synchrotron radiation methods.

strengthening the results, but here only the results of quantitative experimental methods are discussed.

Much the larger number of published solutions of surface structural problems in general[2] have been based on low energy electron diffraction (LEED).[3–5] The strong elastic scattering cross-sections of atoms for low energy electrons ($\sim$30–300 eV), combined with the short inelastic scattering mean-free-path for such electrons in solids, means that it is the natural diffraction technique to probe the structure of the outermost few atomic layers of a solid, potentially filling the dominant role occupied by X-ray diffraction for determining the structure of bulk solids. While visual observation of the low energy electron diffraction pattern provides rather direct information on the surface periodicity (the surface unit mesh), detailed analysis of the diffracted beam intensities as a function of energy (and thus acceleration voltage)—so-called I–V spectra—is required to determine the atomic positions. Relative to conventional X-ray diffraction from bulk crystals, however, a significant complication in the extraction of the structure is the need to model the data through trial-and-error iteration of multiple scattering calculations, a consequence particularly of the large scattering cross-section. Nevertheless, with the huge advances in low-cost high-power computing in the past few years, this type of analysis is no longer a significant barrier to the application of the technique. This more detailed application of the LEED method is usually referred to as LEED I–V analysis or QLEED (quantitative LEED). One important feature of conventional LEED, however, is that it requires long-range order, and indeed if a surface is partly ordered and partly disordered, the diffracted beam intensities derive almost entirely from the ordered regions. This is an important limitation in the investigation of molecular reaction intermediates which commonly do not form long-range ordered structures at surfaces, and for this reason there are actually rather few published QLEED determinations of the structure of such species at surfaces.

Of the many other quantitative probes of surface structure that have been developed in the past 30 years or so, one may identify two with the greatest potential for the *local* structure determination of molecular reaction intermediates at surfaces. These two methods, photoelectron diffraction[6,7] and surface extended X-ray absorption fine structure (SEXAFS),[8,9] both exploit the elastic scattering of the photoelectron wavefield emitted from a core level of an adsorbate atom. In SEXAFS, one selects those scattering events which return the electrons to the emitter atom; the coherent interference between the emitted and scattered components of the photoelectron wavefield at the emitter atom modulates the final-state wavefield amplitude, and this then leads to modulations in the total photoionisation cross-section. Measurements of these modulations in the total cross-section as a function of photon energy provide a relatively direct method to determine the nearest-neighbour bondlengths relative to the emitter atom, while one can investigate the influence of the polarisation direction of the incident X-rays on the modulation amplitudes to obtain limited information on the directions of these near-neighbour bonds. By contrast, in photoelectron diffraction, one detects the photoelectron intensity in a particular direction outside the surface, and it is here at this detector that the interference of the directly emitted and elastically-scattered components of the wavefield occurs. This partial (angle-resolved) measurement of the photoionisation leads to significantly larger interference modulations than in the total (angle-integrated) measurement of SEXAFS, and is certainly one reason why this approach has been more widely used. Moreover, because the scattering paths involved in the interference depend on the direction of photoelectron detection, photoelectron diffraction is more overtly sensitive to the real-space direction of near-neighbour scattering atoms than SEXAFS, and thus to the adsorption site. In principle photoelectron diffraction interference effects, and thus structural information, can be obtained by measuring either the angular distribution of the photoelectrons at fixed energy, or the photoelectron energy dependence at fixed emission directions. The energy-scan mode, commonly given the acronym PhD,[6,7] has been the primary method used for the structures discussed here.

SEXAFS and PhD differ from QLEED in two important ways, namely that they detect the *local* structure around the adsorbed species, and that this structural information is *element specific*. Because the electron source is localised on an adsorbate atom (which may be part of an adsorbed molecule), the scattering process is dominated by the contributions from near-neighbours to the emitter, ensuring that the techniques are relatively insensitive to long-range order in the adsorbate. The characteristic core level binding energies determining the photoelectron energy provide the elemental specificity. Moreover, in the case of photoelectron diffraction, small changes in the photoelectron binding energy—so-called chemical shifts—due to changes in the local electronic environment, allow one to separate out the structural data from atoms of the same element in different local bonding environments. This *chemical-state specificity* has been exploited in PhD studies of molecular adsorbates to distinguish, for example, the local structural environment of the two inequivalent C atoms in a surface acetate species, CH_3COO–, in a largely independent fashion.

One related technique which should probably be mentioned here is NEXAFS—near-edge X-ray absorption fine structure.[10] From an experimental point of view, this is the same as SEXAFS, but focuses on the spectral region within typically 10–20 eV of the absorption edge, an energy range which can also be described in terms of transitions from the core level to intramolecular scattering resonances or transitions to unoccupied electronic states of the molecule. Through the use of simple dipole selection rules it is relatively easy, in many cases, to use the dependence of the NEXAFS spectra on the direction of the polarisation vector of the incident radiation to determine the orientation of a molecular species on a surface. In addition, however, the absolute energies of certain resonances within NEXAFS spectra are dependent on the intramolecular bondlengths. This was first used as a simple empirical monitor of these bondlengths,[11] but far more rigorous theoretical modelling is now being applied to obtain this quantitative structural information. A nice recent example is an investigation of methane physisorbed on Pt(977), in which information on the C–H bondlength was obtained in this way;[12] this is a particularly striking result because H is a weak electron scatterer and in general contributes minimally to LEED,

PhD or SEXAFS. Note also that while LEED and PhD involve electron detection, and thus are generally only applicable in UHV, the X-ray absorption in NEXAFS and SEXAFS can be detected by X-ray fluorescence (resulting from refilling of the core hole), so in this X-ray-in/X-ray-out configuration, these methods can be applied under 'high pressure' conditions.

In the remainder of this review, the results of structure determinations of molecular reaction intermediates on surfaces, determined almost exclusively by one of these three methods, are described. While a brief introduction is included regarding some of the chemistry leading to the formation of these species, the focus here is on the structural solutions, and not on the chemistry that motivates interest in them. Notice, incidentally, that none of the structural methods used in these studies are capable of determining the position of H atoms within these molecular species. H has no true atomic core level, and so cannot be used as the electron source in photoelectron diffraction or SEXAFS, and it is an extremely weak scatterer of low energy electrons, thus having a minimal influence on the scattering interferences involved in all of these techniques (although, as remarked above, it seems that it can be detected, at least in some cases, in NEXAFS). In the illustrations of the adsorbed structures that follow, therefore, H atom positions are schematic only, and were not determined experimentally.

2. Formate and methoxy species on copper surfaces

The two molecular surface reaction intermediates that seem to have been most studied structurally are formate (HCOO–) and methoxy (CH_3O–), which can be formed by simple deprotonation from formic acid (HCOOH) and methanol (CH_3OH) on a number of (mainly metal) surfaces. On copper surfaces, at least, both species have been identified in investigations of the catalytic oxidation of methanol which can proceed by two main routes, one a valuable mechanism for producing formaldehyde (H_2CO), while the alternative combustion route produces only H_2O and CO_2. It seems to be generally accepted that formaldehyde is produced from the adsorbed methoxy intermediate, the formation of which is strongly enhanced by the presence of surface oxygen, leading to a suggested process:

$$CH_3OH_{ad} + O_{ad} \rightarrow CH_3O_{ad} + OH_{ad}$$

$$CH_3O_{ad} \rightarrow H_2CO + H_{ad}$$

while the alternative combustion route is suggested to involve the formate intermediate:

$$CH_3O_{ad} + O_{ad} \rightarrow HCOO_{ad} + 2H_{ad}$$

$$HCOO_{ad} \rightarrow CO_2 + H_{ad}$$

However, the formate species has also been identified as a surface intermediate in the water–gas shift reaction (the production of H_2 and CO_2 from CO and water, *e.g.* ref. 13), and, indeed, in the reverse reaction of photoreduction of CO_2 with H_2 to CO, on a number of surfaces, mainly of transition metals and transition metal oxides. Moreover, methoxy is regarded as an important surface intermediate in the catalytic production of methanol.

The first structural study of these species was an O K-edge SEXAFS investigation of the formate species on Cu(100), in which the polarisation-direction dependence of the near-edge X-ray absorption structure (NEXAFS), the energy range in which intramolecular scattering effects dominate the spectra, provided information on the molecular orientation.[14,15] The NEXAFS data indicated that the molecular plane lies perpendicular to the surface. However, the interpretation of the SEXAFS data led to the conclusion that the molecule occupies a cross-bridging site (with the O–O direction parallel to the surface but perpendicular to the Cu–Cu nearest neighbour direction within the surface) such that the two O atoms occupy off-hollow sites on the surface (see Fig. 1). This geometry, with a surprisingly large Cu–O nearest neighbour distance of 2.38 Å, was heralded as the first example of a new type of molecule–surface bond; *i.e.* that the bonding to an extended metal surface was fundamentally different from the bonding to metal atoms in metal coordination compounds. Such a conclusion is surely interesting, but it turned out to be incorrect, the mis-interpretation of the SEXAFS data apparently arising from a failure to take account of the role of intramolecular O atom backscattering, assuming, instead, that only Cu substrate scattering was important. This error was revealed as a result of subsequent SEXAFS experiments to investigate the formate species on Cu(110),[16,17] followed by a PhD investigation of the formate species on both surfaces and reconsideration of the earlier SEXAFS data.[18] The resulting conclusion was that on both surfaces the formate adopts an aligned bridge geometry such that each carboxylate O atom is near atop one of the two nearest neighbour surface Cu atoms, with Cu–O bondlengths of a little less than 2.0 Å (Fig. 1). This final

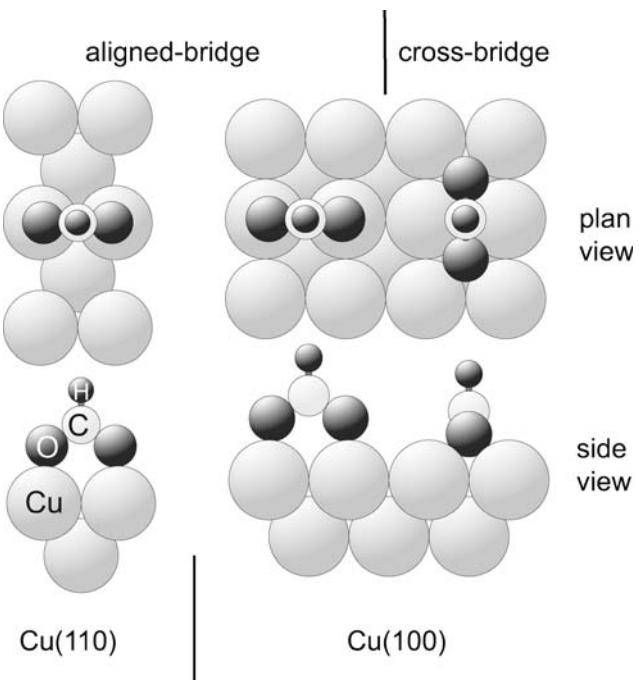

Fig. 1 The local aligned-bridge adsorption sites of the formate (HCOO–) species on Cu(110) and Cu(100). Also shown is the cross-bridge site on Cu(100) originally proposed as a 'new type of surface bond' but subsequently shown to be incorrect.

structural conclusion, of course, means that the geometry of the formate–Cu surface bonding on both (100) and (110) surfaces is actually very similar to that found in coordination chemistry, and is *not* some new type of bonding. Specifically, both the local metal–formate geometry and the associated Cu–O bondlengths are closely similar to those found in several copper formate complexes.[19–22] This re-interpretation of the adsorption geometry of formate on Cu(100) has also been supported by the results of cluster calculations.[23] More recently, an investigation of the local structure of the formate species on Cu(111),[24] using a rather different technique of normal incidence X-ray standing waves (NIXSW), concluded that a similar aligned-bridge bonding geometry is also adopted on this surface.

In contrast to the bonding of the formate species on these three low index faces of copper, in which the O atoms occupy singly-coordinated Cu sites, the methoxy species bonds to Cu surfaces through the O atom in more highly-coordinated sites. On Cu(111), in particular, a PhD investigation identified the adsorption site as the 'fcc' three-fold coordinated hollow, directly above a third-layer Cu atom with a Cu–O bondlength of 1.98 Å.[25] Three-fold coordinated hollow sites were also identified in an independent NIXSW study of this system, although in this case co-occupation of the fcc hollows and the hcp hollows (directly above second layer Cu atoms) was preferred.[26] These studies of the methoxy species on Cu(111) were actually predated by investigations on Cu(100) and Cu(110), although the results are more surprising. In the case of the Cu(100) surface, an early PhD investigation favoured a geometry in which the O bonding atom occupies a site that is displaced laterally from the four-fold symmetric hollow site to a location that is only two-fold coordinated.[27] This slightly surprising conclusion could, perhaps, be a consequence of the small data set and the simplified theoretical treatment used in the data analysis, but it is interesting to note that a slightly earlier O K-edge SEXAFS study[28] had been interpreted in terms of a mixture of hollow and bridge sites, but could equally well be accounted for by this single intermediate site. Interestingly, NEXAFS data collected at the O and C K-edges led to conflicting information concerning the orientation of the C–O intramolecular axis, consideration of both data sets leading to the conclusion that an orientation within 10° of the surface normal was the more likely interpretation than a tilt of ~28°.[27] There has been no equivalent fully-quantitative structural study of the Cu(110)/methoxy system, but in this case a conclusion from NEXAFS measurements that the O–C intramolecular bond directions are significantly removed from the surface normal[29] was also supported by high-energy angle-scan photoelectron diffraction measurements,[30] albeit with different detailed interpretation in the tilt directions. This led to a tentative suggestion that on this surface, too, a low-symmetry (possibly three-fold coordinated) adsorption site may be occupied. It would certainly be interesting to investigate the (100) and (110) surfaces further to establish the extent to which the methoxy–Cu coordination does vary on the three low index faces of Cu.

3. Other carboxylate, alkoxy, and related studies

While the formate and methoxy species on copper surfaces were the subject of the first quantitative structural studies of molecular surface reaction intermediates, there have been quite a number of more recent investigations of carboxylate species, and of methoxy on other surfaces. Almost all of these have been on metal surfaces, and, indeed, predominantly on copper, but one rather different example is that of the formate species on rutile TiO_2(110). As on the Cu surfaces discussed in the previous section, the surface formate studied in the UHV structural studies has been formed by deprotonation of formic acid on the clean surface, but whereas on metal surfaces the acid H atom leads to chemisorbed atomic H species, which combine at an appropriate temperature to lead to the desorption of H_2, on an oxide surface the acid H atom can bond to a surface O atom to form a local hydroxyl species.

The TiO_2(110)/HCOO + H system has been investigated structurally in two independent studies,[31–33] both based on photoelectron diffraction (angle-scan and energy-scan), and both exploiting the chemical shift in the photoelectron binding energy of the O 1s state between the oxidic (substrate) and adsorbate O atoms. This shift, of ~1.6 eV, allows one to collect photoelectron diffraction data from the adsorbate O atoms alone. One complication, however, is that it appears that the O 1s chemical shift associated with the O atoms in the adsorbate formate species is essentially identical to that of the O atoms in the OH species produced by the acid H atoms, so the photoelectron diffraction data obtained from this chemically-shifted O 1s emission actually comprises an incoherent sum of the diffraction from the two species. In the earlier study,[31,32] this complication was not appreciated, but nevertheless the later investigation[33] confirmed the originally-identified adsorption site of the formate species, but provided more complete and accurate identification of the complete geometry. On the clean TiO_2(110) surface, in the unreconstructed (1×1) phase, there are two undercoordinated atomic sites at which adsorption and reaction may be favoured. These are the surface Ti atoms (five-fold coordinated to O, as opposed to six-fold coordinated in the bulk) and the surface bridging O atoms (two-fold coordinated to Ti as opposed to three-fold in the bulk). The formate species is found to bridge-bond to an adjacent pair of five-fold coordinated Ti atoms in a geometry quite similar to that adopted relative to Cu atoms on the low index faces of metallic Cu. The mismatch of the surface Ti–Ti distance (2.96 Å) on the surface, to the O–O distance (2.21 Å) of an unstrained formate species, is significantly greater than that of the Cu–Cu distance (2.56 Å) on the Cu surfaces, but this bidentate bonding still appears to be preferred. Independent evidence that the molecular plane lies perpendicular to the surface and preferentially aligned along the azimuthal direction corresponding to the Ti–Ti nearest-neighbour distance came from NEXAFS[34] and polarisation-angle-dependent infra-red spectroscopic studies,[35] although these experiments found some evidence for a second, azimuthally-rotated, species that may be associated with monodentate formate bonding at bridging oxygen vacancy sites on the surface. The experimentally-determined structure of the TiO_2(110)/HCOO + H surface (Fig. 2) is actually in excellent agreement, both in adsorption sites and chemisorption bondlengths, with the results of a DFT calculation.[36] Note that, as may be expected, the atomic H causes hydroxylation of the undercoordinated bridging O atoms.

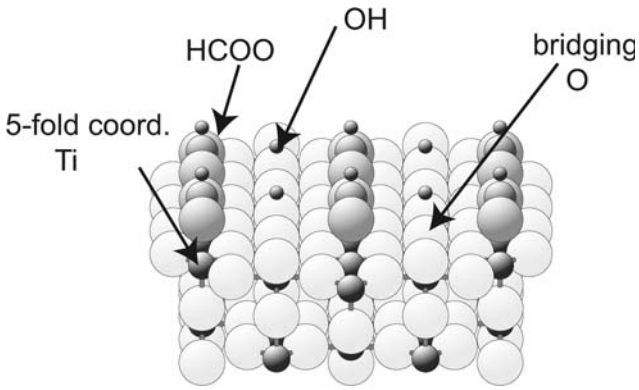

Fig. 2 The structure of the coadsorbed formate and atomic hydrogen (to form surface hydroxyl species) on TiO_2(110), also showing the undercoordinated Ti and O sites in the surface.

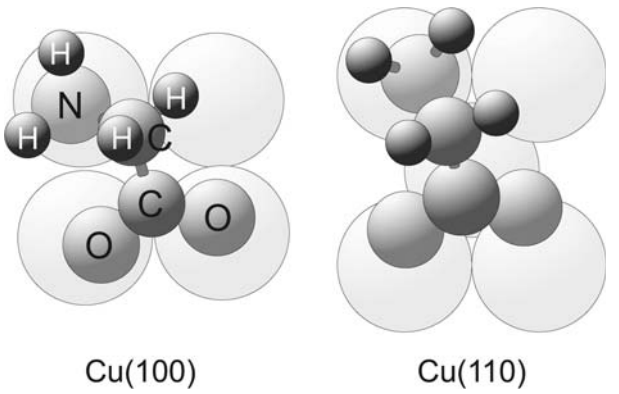

Fig. 3 Plan views of the local geometry of glycinate (deprotonated glycine, NH_2CH_2COO) on Cu(100) and Cu(110).

It is perhaps worth remarking that on oxide surfaces it is generally believed that surface hydroxyl species play an important role in many chemical processes. Indeed, such species may be ubiquitous on oxide surfaces in 'real' working environments and, of course, at interfaces with aqueous solutions. On TiO_2(110), much the most investigated of all oxide surfaces, this investigation of hydroxy species in the presence of coadsorbate formate seems to be the only structural study. Very recently, one further structure determination of a hydroxylated oxide surface, namely V_2O_3(0001), also using the chemical-state-specific PhD technique, has been published;[37] here, too, hydroxylation appears to occur at undercoordinated surface O sites, but not, apparently, at terminating vanadyl (V═O) sites that are believed to be present on this surface.

Returning to metal surfaces, other structural studies of deprotonated carboxylic acid species include acetate (CH_3COO–) on Cu(110)[38] and Cu(111),[39] and benzoate (C_6H_5COO–) on Cu(110);[40] in all cases the molecular plane lies perpendicular to the surface with symmetric bidentate bonding of the two O atoms in bridge sites, exactly as for the formate species.

A somewhat different class of carboxylate adsorbates that has been studied structurally is the dehydrogenated amino acids. In this case, of course, one might question whether these species really fit naturally into a review of surface reaction intermediate species. Certainly they are species that are only present on the surface, and the deprotonation does represent a surface reaction, but one may question whether they act as important intermediates in any subsequent reaction of chemical interest. Rather, the surface reaction (deprotonation) provides a mechanism for the attachment of the molecule to the surface in a similar way that the deprotonation of thiols (particularly simple alkane thiols) is a necessary condition to produce self-assembled monolayers (SAMs) of thiolates on the surfaces of noble metals, and especially of Au(111) (systems that are much-studied in general,[41,42] and which have also been subjected to some quantitative structural studies, *e.g.* ref. 43). However, of the fully-quantitative structural studies of deprotonated amino acids on surfaces, namely of glycine on Cu(110)[44,45] and Cu(100),[45] and alanine on Cu(110),[46] it is interesting to note that these are carboxylates that do *not* 'stand up' on the surface, but rather adopt an orientation that allows attachment to the surface not only through the two carboxylate O atoms, but also through the amino N atoms. Fig. 3 shows a schematic diagram of the local bonding geometry of the glycinate species, NH_2CH_2COO, on the Cu(100) and Cu(110) surfaces. In both cases the bonding is through both O atoms and the N atom, all in off-atop (singly-coordinated) sites relative to the outermost layer Cu atoms, although on Cu(110) the larger spacing of the close-packed Cu atom rows, relative to the size of the molecule, leads to the amino N atom being close to atop but the carboxylate O atoms to be significantly displaced laterally from atop sites. As indicated in Fig. 3, the different substrate structure and the associated chemisorption constraints is also likely to lead to some difference in the internal molecular conformation, but in the absence of any explicit information on the C atom sites, this effect has not been quantified. The local geometry adopted by alaninate, NH_2CHCH_3COO, on Cu(110) is very similar, although the nature of the long-range ordering proves to be of considerable interest, because glycinate adopts a structure containing glide symmetry, whereas alanine is chiral and so cannot do so in a single enantiomer.

In the same way that there is a consistent pattern of all these carboxylates adopting bidentate surface bonding on this range of different surfaces, at least in the specific structural phases that have been investigated in detail, structural studies of the methoxy species on Ni(111) and Al(111) favour three-fold coordinated hollow sites, as on Cu(111). There is, however, one curious variation. On Cu(111), as reported in the previous section, PhD experiments clearly favour bonding of the O atom to the fcc hollow site, atop a third layer Cu atom, and this same technique yields the same result for methoxy on Ni(111).[47] By contrast, on Al(111), a NIXSW study found clear evidence for occupation of the hcp hollow site, directly above a second layer metal atom.[48] In general, these two sites differ only in either the second- or third-nearest neighbour distances (depending on the adsorbate–substrate interlayer spacing) and so may be expected to have closely similar adsorption energies. Nevertheless, in most atomic and molecular adsorbates that adopt these hollow sites, the fcc sites appear, in practice, to be preferred. In some adsorption systems, co-occupation of both sites occurs at higher coverages, but this is also consistent with the notion that there is a small adsorption energy difference. Indeed, one possible

reason for the apparent discrepancy between the results of the PhD and NIXSW experiments performed on methoxy on Cu(111), which favour, respectively, fcc hollows and both hollows, is that the coverage was higher in the NIXSW study. In this regard it is notable that the methoxy coverage achieved on a Cu surface does depend on the precoverage of atomic O, before exposure to methanol. Both too little and too much preadsorbed O can lead to sub-saturation coverage of methoxy. Nevertheless, none of this accounts for the unusual preference for the hcp site shown by methoxy on Al(111), although this situation is not unique, as will be shown in the following section.

Finally, within this section, it is appropriate to mention work on the surface carbonate species, CO_3, which has been implicated as a surface intermediate in a range of reactions involving carboxylates and alkoxy species, including formic acid oxidation and methanol synthesis (*e.g.* ref. 49) as well as the water–gas shift reaction.[13] The only quantitative structure determination of a surface carbonate species is a PhD investigation on the Ag(110) surface,[50] the carbonate being produced by oxidation of CO_2 on an oxygen pre-dosed surface. As shown in Fig. 4, the molecular plane lies near-parallel to the surface with one of the O atoms bridging a pair of nearest-neighbour Ag atoms in an adatom row. The existence of these Ag adatom rows (*i.e.* an 'added row' structure, equivalent in the static structure to the effect of 'missing rows') may be inferred from the (1×2) LEED pattern, but are also clearly seen in STM images of this surface.[51,52] Indeed, the general location of the carbonate species is also consistent with STM images which do not, of course, provide any quantitative detail regarding the structure. The adsorption geometry found experimentally is also in excellent agreement with the results of a later DFT calculation,[53] and the exact atomic coordinates shown in Fig. 4 correspond to those found in this calculation. The only significant difference between this geometry and the optimised one found in the PhD experiment is in the molecular tilt; the experiment found the molecular plane to be almost exactly parallel to the surface such that the two O atoms that are not bridging the adatom row appeared to be rather far from underlying Ag atoms. Because the PhD investigation relied entirely on C 1s photoemission data, the ability to determine the relative location of the O atoms relies on the intramolecular scattering. This proved surprisingly sensitive to the azimuthal orientation of the molecule, but is not very sensitive to the tilt. Interestingly, earlier NEXAFS studies[54,55] had also indicated that the molecular plane is parallel to the surface, but with an estimated precision of only ±15°. As may be seen in Fig. 4, the molecular tilt angle of 20° found in the DFT calculations allows the molecule as a whole to lie closer to the (111) 'nanofacet' formed on the surface by the added Ag atom row, and thus for all the O atoms to be in the range of Ag–O bonding distances, which makes for a more rational structure. The fact that one oxygen is bridging the Ag adatoms, but the other two O atoms are in off-atop sites, means the molecular tilt angle is significantly less than that of the (111) nanofacet (35°).

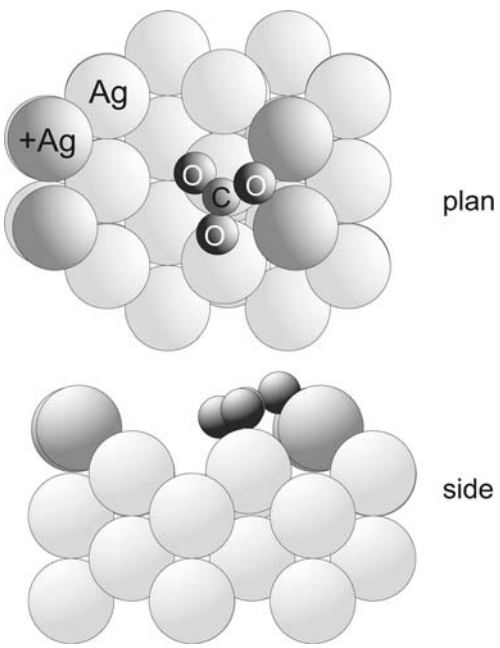

Fig. 4 The local structure of the carbonate, CO_3, species on Ag(110). Atoms labelled '+Ag' are in rows of Ag adatoms on the bulk-terminated Ag(110) structure.

4. Hydrocarbons

While there have been a number of quantitative structural studies of adsorbed hydrocarbon molecules on surfaces, most of these are of the intact gas-phase species, and not the result of a surface reaction. One example that straddles the dividing line of this classification is the study of adsorbed ethylene, C_2H_4, and acetylene, C_2H_2, on Ni(111). This is because ethylene, adsorbed on Ni(111) at low temperature, dehydrogenates to produce adsorbed acetylene as the surface is warmed towards room temperature; this system provided the first example of the use of a 'modern' surface science technique, namely ultraviolet photoelectron spectroscopy, to follow *in situ* a simple surface reaction on a single-crystal surface.[56] Thus while acetylene is a gas-phase molecule, adsorbed on Ni(111) it is also a reaction intermediate in the dehydrogenation of ethylene. Unfortunately, it is not a particularly useful catalytic reaction chemically, because further heating results not in the desorption of the acetylene, but in further dissociation to leave a carbon residue on the surface, although there appears to be an intermediate stage involving C–C bond scission to leave CH species on the surface.[57] Nevertheless, this simple dehydrogenation reaction is one process that it is possible to follow in detail with UHV surface science methods, so it is interesting to know the local structure of the adsorbed ethylene and acetylene on this surface, the initial and final stages of the reaction. The PhD technique has been applied to this problem,[58,59] and the local adsorption geometry of the two species found in this study are shown in Fig. 5. Notice that at the dissociation temperature of adsorbed ethylene (~230 K), the acetylene product is coadsorbed on the surface with atomic H, but the presence of this coadsorbate appears to have no detectable influence on the local geometry of the adsorbed acetylene. One interesting finding of the structural study is that the two C atoms in the adsorbed acetylene are located exactly

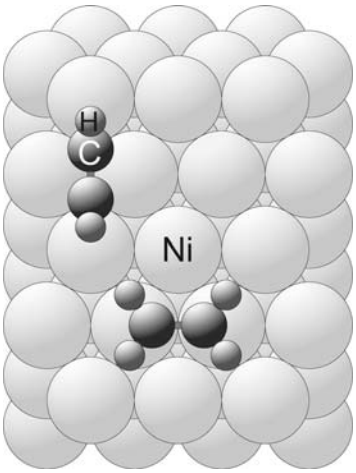

Fig. 5 Plan view of the local structure of acetylene, C_2H_2, and ethylene, C_2H_4, on Ni(111).

(to within the precision of the measurement) in the two (fcc and hcp) hollow sites of the surface. This leads to a C–C bondlength of 1.44 Å, very substantially longer than in gas-phase acetylene (1.21 Å). The reduction in the C–C bond order implied by this bondlength change is also consistent with a strong softening of the C–C stretching vibration found in vibrational spectroscopy.[57] As such, this surface species is really a strongly modified form of acetylene as a result of its interaction with the surface. Part of the motivation for this structural study was to try to understand the geometrical reaction path from reactant to product. Evidently the two rather different adsorption sites, with acetylene in the cross-bridge geometry and ethylene in the aligned bridge site, must involve some azimuthal rotation of the C–C, possibly accompanied by translation. Of course, this simple picture implies that the loss of the two H atoms is coordinated; in reality, there may well be a short-lived intermediate stage in which only one H is lost.

In this context, it is interesting that on some other transition metal surfaces ethylene adsorption does result in the formation of a stable species, ethylidyne (CCH_3), involving the loss of only a single H atom. The structure associated with this species, in an ordered (2×2) phase, has been determined by QLEED on both Pt(111)[60,61] and Rh(111).[62–64] The Rh(111)(2×2)–CCH_3 structure is shown schematically in Fig. 6. The molecule bonds to the surface in a three-fold

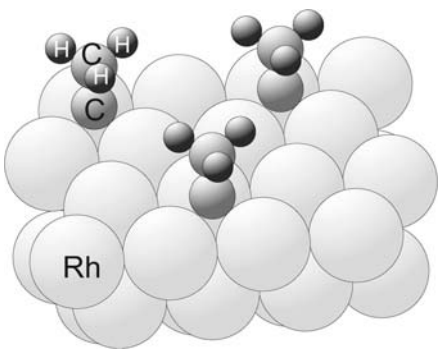

Fig. 6 The structure of the Rh(111)(2×2)–CCH_3 surface phase.

coordinated hollow site with the C–C axis perpendicular to the surface. There is, however, an interesting difference between the two substrates, in that on Pt(111) the molecule lies in fcc hollow sites, whereas on Rh(111) it occupies the hcp hollows. This subtle difference is similar to the case of the methoxy species on the (111) surfaces of Cu, Ni and Al discussed in the previous section. There seems to be no real understanding of the unusual behaviour of the Rh(111)/CCH_3 and Al(111)/CH_3O-systems in showing a clear preference for the hcp hollow sites. The Rh(111)/CCH_3 is particularly curious as a QLEED study of a CO–CCH_3 coadsorption phase on Rh(111) led to the conclusion that the ethylidyne then occupies the fcc hollows with the CO in the hcp hollows,[65] although in a NO–CCH_3 coadsorption phase on the same surface ethylidyne is found in the hcp hollows with NO in the fcc hollows.[65]

The only other example of a structure determination of a hydrocarbon species on a surface resulting from a surface reaction seems to be a very recent PhD investigation of a C_3H_3 species on Pd(111)[66] resulting from the dissociation of furan, C_4H_4O, into coadsorbed C_3H_3 and CO. The presence of this species on the surface has been inferred from electron and vibrational spectroscopy, together with conventional and laser-induced thermal desorption (LITD).[67–69] Interestingly, the LITD experiments also showed evidence of some C_3H_3 coupling to produce benzene, although molecular benzene is not seen in conventional thermal desorption spectra as benzene dissociates on Pd(111) on heating. Bearing in mind the picture of a C_3H_3 species as one half of a benzene molecule, one might expect a triangular structure with bonding to the surface through a pair of C atoms and an orientation of the molecular plane approximately perpendicular to the surface, and indeed this is, rather approximately, the structure adopted by a methylated version of this species, with the $(CCH_3)_3$ species bonded to three Ru atoms in the organometallic complex $(\mu\text{-H})Ru_3(\mu_3\text{-}\eta^3\text{-CMeCMeCMe})(CO)_9$.[70] For the surface C_3H_3 species, the preferred structural solution does, indeed, have two C atoms in sites off-atop Pd atoms in a geometry similar to that in the Ru complex, but the molecular plane is much more nearly parallel to the surface than seen in this organometallic analogue. This is certainly an example for which the application of DFT calculations could prove illuminating.

5. Nitrogen-containing species

Of all catalytic processes involving nitrogen-containing species, almost certainly the most important is the Haber process for the production of ammonia from gaseous nitrogen and hydrogen, a process that transformed agriculture and food production in the 20th century. Understanding the mechanisms and rate-limiting steps in this process has been one of the key goals in modern surface science and one to which Ertl and co-workers have made major contributions. Important in this process are the various NH_x surface species that are also seen in the fragmentation of ammonia on active surfaces (*e.g.* ref. 71). Despite the many surface science studies identifying these surface reaction intermediates, however, there have been very few quantitative structural studies of these species, and indeed none on the surfaces of materials most relevant to the

Haber process. Instead, there have been structure determinations of NH_x intermediates formed through reaction with gas-phase ammonia on Cu(110), Si(100) and Si(111), the main practical motivation for silicon surface studies being the formation of nitride interfaces in semiconductor device processing.

In the case of the investigation on Cu(110), the study was motivated by prior studies of oxy-dehydrogenation of ammonia by oxygen that identified, under different conditions, a surface amide (NH_2) and a surface imide (NH);[72,73] specifically, exposure of preadsorbed ammonia to molecular oxygen at low temperature was believed to yield the surface amide, while exposure of the clean surface to an ammonia-rich NH_3–O_2 gas mixture at room temperature yielded the surface species identified as the imide. The N 1s PhD structural study[74] was conducted on a surface prepared in the latter fashion (using an $NH_3 : O_2$ partial pressure ratio of 36 : 1), and was thus believed to produce the imide species. The key conclusion of this investigation was that the N atom occupies a short bridge site, midway between two nearest-neighbour surface Cu atoms along the ⟨110⟩ close-packed direction, with a Cu–N bonding distance of 1.89 Å. This multiply-coordinated (two-fold) adsorption site is, of course, broadly consistent with the loss of H atoms from the NH_3 molecule which typically bonds atop surface atoms in a one-fold coordinated geometry, a situation found on Cu(111),[75] Ni(111),[76] and Ni(100).[77] Curiously, on Cu(110), NH_3 appears to adopt a low-symmetry off-atop site,[78] although the one-fold coordination is retained. The longer Cu–N bondlength for ammonia adsorption (2.09 Å on Cu(111) and 2.04 Å on Cu(110)) relative to that of the imide adsorption on Cu(110) is also qualitatively consistent with the modified Cu–N bond order to be expected.

On Si surfaces, of course, adsorbate bonding is strongly influenced by the presence of 'dangling bonds' that reflect the local directional covalent bonding of the bulk solid. On both Si(100) and Si(111), the clean surfaces undergo substantial reconstruction to reduce the number of dangling bonds relative to those of ideal bulk termination of the solid. Nevertheless, some dangling bonds remain, and adsorbates may cause modifications to these reconstructions as the dangling bonds become saturated by adsorbate bonding. In the case of the Si(100) surface, an unreconstructed bulk termination would lead to each surface Si atom having two of its four Si–Si bonds unsaturated, and adjacent pairs of atoms move together to form dimers, reducing the number of dangling bonds per surface atom from two to one. On this reconstructed surface the dimers are actually asymmetric, with one Si atom lower on the surface than the other, but at room temperature these dimers flip dynamically between the two alternative asymmetries, leading to an average (2×1) periodicity. Even at low temperature, exposure to ammonia is found to lead to reaction to form coadsorbed NH_2 and atomic H species, that are believed to bond to the two dangling bonds at opposite ends of the Si surface dimers. A PhD structural study of this surface[79,80] substantially confirms this picture, although as in all the studies discussed here, the locations of the H atoms were not determined. However, the PhD experiments show that the N atoms do bond in an off-atop location relative to surface Si atoms with a Si–N bondlength of 1.73 Å and an angle of this bond relative to the surface normal of 21°,

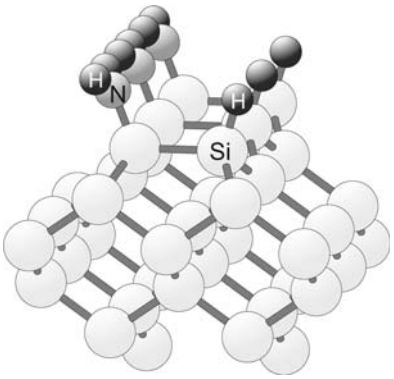

Fig. 7 Schematic diagram of the structure of coadsorbed NH_2 and H on Si(100) as a result of interaction of the clean surface with NH_3. Note that, as in the other studies reported here, the location of the H atoms is not determined experimentally, while it is not certain that the NH_2 and H species on the two ends of the Si surface dimers are as well-ordered as implied by this diagram.

all consistent with attachment to a Si surface dangling bond (Fig. 7). The experimental study also shows that the Si–Si dimer remains intact, but becomes significantly less asymmetric (and possible symmetric).

On Si(111), the situation is substantially more complex. The clean surface reconstructs to a (7×7) periodicity, thus involving major reorganisation of the surface layers. Fig. 8 shows a schematic diagram of the dimer–atom-stacking fault (DAS) model first proposed by Takayanagi *et al.*[81] on the basis of high energy electron diffraction data, which is now accepted as correct. On an ideal bulk-terminated Si(111) surface there would be one dangling bond per surface Si atom (perpendicular to the surface), each such atom being bonded to three Si atoms in the layer below. This would lead to 49 dangling bonds per (7×7) surface unit mesh. This is reduced by two main mechanism. Firstly, as on the Si(100) surface, some pairs of surface Si atoms move together to form dimers, removing the dangling bonds from these atoms. In Fig. 8 these dimers are seen around the edge of the diagram and on the vertical line dividing the unit mesh in two. The second key process

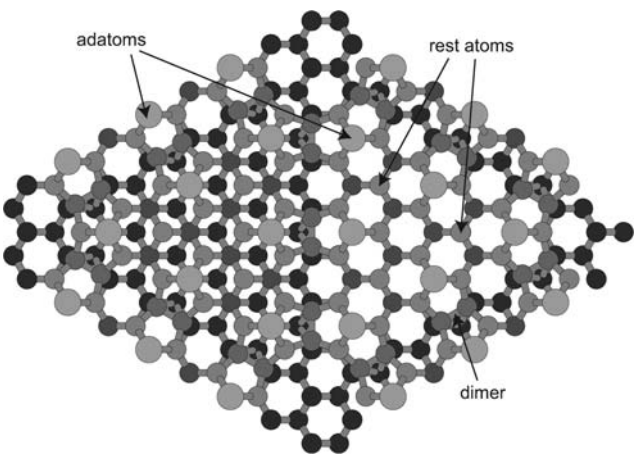

Fig. 8 Plan view of the Si(111)(7×7) 'DAS' clean surface structure. The different atomic radii and levels of grey shading correspond to different layers in the near-surface region.

reducing the number of dangling bonds is the attachment of Si adatoms at the centres of triangular groups of three adjacent Si atoms in the surface. This has the effect of removing the three dangling bonds from this group of three atoms, but leaves one dangling bond at the adatom. A final feature of the reconstruction that results in overall energy lowering is reflected in the different appearance of the left and right hand halves of the diagram of Fig. 8 that is a consequence of a near-surface stacking fault in the left-hand half of the unit mesh. Inspection of this figure shows that within the unit mesh there are 12 Si adatoms, each having a dangling bond, but there are also 6 'rest atoms', the dangling bonds of which are unaffected by the reconstruction. In fact there is also one 'corner hole' Si atom, located at each of the corners of the unit mesh shown in Fig. 8, that also retains its dangling bond, so the effect of the reconstruction is to reduce the number of dangling bonds per surface unit mesh from 49 to 19. Evidently, these remaining dangling bonds are the preferred sites for adsorption in the absence of adsorbate-induced reconstruction.

Adsorption of NH_3 on Si(111) also leads to sequential deprotonation at increasing temperatures, with the initial stage, to produce adsorbed NH_2, occurring at temperatures as low as 100 K, although on the (111) surface, unlike the (100) surface, there is some evidence that NH species are already present on the surface at room temperature.[82–84] A relatively recent PhD structural study of the Si(111)/NH_3 adsorption system,[85] performed at room temperature, was undertaken with the objective of identifying the preferred adsorption sites of the NH_x species. The spectral resolution of this investigation was inadequate to formally distinguish the possible presence of both NH_2 and NH species on the surface (which do lead to slightly different N 1s photoelectron binding energies[84]). The key conclusion was that the NH_x species, believed to be entirely or predominantly NH_2, are adsorbed atop the Si rest atoms (with a Si–N bondlength of 1.71 ± 0.02 Å), with no more than a small minority adsorbed atop the Si adatoms. One may surmise that these adatom sites are where the H atoms from the NH_3 fragmentation are bonded.

One further N-containing surface species that has been the subject of several quantitative structure determinations is that of the cyanide, CN, species that is often studied as the simplest model system for the adsorption of organic nitriles. In general, the surface CN species has been formed by the dissociation of cyanogen, C_2N_2, and indeed part of the interest in the surface chemistry of this species stems from its relevance to chemical warfare and ways to counteract the impact of such activity. A further issue of particular practical importance, that is of more general importance, is the identification of a CN-containing surface intermediate in the reaction of CO with N_2 and NO,[86–88] raising the spectre of poisonous HCN production in three-way automotive exhaust catalysts. More generally, the fact that CN^- is isoelectronic with CO, and that there is some analogy in the coordination chemistry of these two species, has added a further motivation to these studies. In this context, one particularly interesting feature of CN adsorbed at surfaces is an apparent systematic difference between the behaviour at solid/vacuum and solid/liquid interfaces. Studies of the cyanide species, CN, at metal–solution and electrode–electrolyte interfaces have been motivated in part by its relevance to electroplating, and in part by its identification as a surface intermediate in the oxidation of amino acids (*e.g.* ref. 89). At these solid/liquid interfaces there is a general consensus, based on vibrational spectroscopic data, that the CN adsorbs with its molecular axis essentially perpendicular to the surface, bonding through the C end (*e.g.* ref. 90–93), in much the same way that CO is found to adsorb at almost all solid/vacuum interfaces. By contrast, CN at solid/vacuum interfaces appears to adopt an orientation in which the C–N axis is much more nearly parallel to the surface. This distinction may well be related to the different role of covalent and ionic bonding in the two situations, combined with the effect of the electrostatic field at the solid/electrolyte interface.

Much the most complete structural studies of CN adsorbed at the solid/vacuum interface are those of the ordered c(2×2)–CN overlayer phases found on the fcc (110) surfaces of Ni [94–96] and Rh.[97] On Ni(110) the original structure determination was based on C and N 1s PhD measurements,[94] subsequently confirmed by a QLEED study,[96] with some supplementary information from medium energy ion scattering.[95] On Rh(110) the structure determination was based on QLEED. The molecular orientation of CN in the Pd(110)c(2×2)–CN phase has also been investigated by NEXAFS and angle-scan photoelectron diffraction,[98] leading to results that strongly suggest the local adsorption site is similar to that on the Ni and Rh surfaces. In these systems the CN lies above second layer substrate atoms with its molecular axis in the [001] azimuth such that it straddles a pair of close-packed substrate atoms rows. The C atom lies slightly lower on the surface such that this atom is three-fold coordinated to two outermost layer and one second layer substrate atoms, whereas the N atom is two-fold coordinated to adjacent outermost layer atoms (Fig. 9). This leads to a tilt of the C–N axis out of the surface which falls in the range 18–25° for these three different substrates. In addition, spectroscopic data (mainly high-resolution electron energy loss spectroscopy—HREELS) have been interpreted as indicating that CN adsorbs with its molecular axis essentially parallel to the surface on Pd(100),[99,100] on Ru(0001)[101] and on Cu(111).[102] However, it is only on the last of these surfaces, Cu(111), that there has been an attempt to determine the local adsorption site, in this case by PhD (supplemented by a NEXAFS

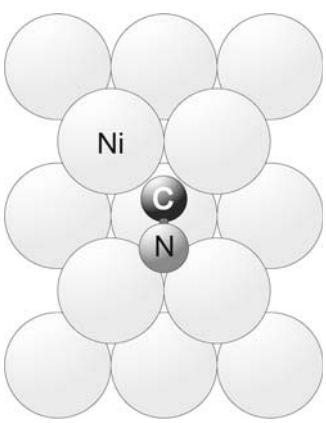

Fig. 9 Schematic diagram of the local adsorption geometry of CN on the Ni(110) surface in the ordered c(2×2) phase.

determination of the molecular orientation). In this case it appears that the C–N axis is closely parallel to the surface, but the best-fit adsorption geometry to model the PhD data corresponds to a low symmetry adsorption site with the CN lying slightly displaced from the 3-fold coordinated hollow sites but with the C and N atoms having single Cu atom nearest neighbours at distances of 1.98 ± 0.05 Å and 2.00 ± 0.05 Å, respectively. This geometry is closely similar to that found in a subsequent DFT calculation.[103]

6. Other species and general remarks

One further species that has been the subject of some surface structural studies but does not fit into any of the above categories is the SO_3, sulfite, species. There have been quite a number of investigations of the interaction of SO_2 with surfaces, for which there is a clear underlying interest related to atmospheric pollution and 'acid rain', associated with S-containing contaminants in fossil fuels, and particularly in the burning of 'brown coal' in power stations in some geographical regions. Various such studies have identified SO_x surface intermediates, including SO, SO_3 and SO_4 (*e.g.* ref. 104). While there are quite a number of structural studies of the intact SO_2 molecule on surfaces, the only equivalent investigations of reaction intermediates are of species identified as SO_3 on Cu(100),[105] Cu(111),[106] and Ni(111)[107] for which, in each case, S K-edge NEXAFS established that the C_{3v} symmetry axis is essentially perpendicular to the surface. Interestingly, in all of these structural studies, based for Cu(100) on SEXAFS data, and for the two (111) surfaces, on NIXSW data, the conclusion is that the molecule adopts a pyramidal structure with the O atoms significantly closer to the surface than the S atoms, although the local lateral registries differ. On Cu(100) and Ni(111) the favoured geometry places the S atom over a bridging site between two nearest-neighbour metal surface atoms, while on Cu(111) a geometry in which the S atom lies atop a surface Cu atom is found. Interestingly, DFT calculations[108] reproduce the experimental result on Ni(111), but favour a similar bridging site on Cu(111); these calculations, however, did expose some problems in addressing the bonding of SO_2 to Cu(111), so it is not clear how significant is this discrepancy with experiment.

As remarked upon several times earlier, in compiling this review it has not been trivial to define its boundaries. The general definition of surface reaction intermediates as species that do not exist naturally in the gas phase includes, for example, atomic C, N and O which all play important roles in surface catalytic processes. Introducing the constraint of molecular species has significantly narrowed the range, not least because the number of quantitative structural studies of molecules on surfaces is already quite modest. Finally, one might ask the question, 'intermediate to what?'. This review certainly does not cover exhaustively all molecular adsorbates that are deprotonated by interaction with the surface; most notably, there is no detailed presentation of the work on deprotonated alkyl thiols; as mentioned in section 3, most of these surface reactions serve only to bind the molecule to the surface, and not to create surface species that play a subsequent role in catalytic reactions, although arguably in some cases they may relate to desulfurisation mechanisms. Similar arguments might be used to exclude deprotonation of some carboxylic acids (such as the amino acids), yet here the natural development of trends from species such as formate, which surely does fall firmly in the topic of this review, seemed to call for some discussion of this work.

What is clear, however, is that the extent and range of the structural work so far is quite narrow. A few trends are clear. Most (probably all) molecule–surface bonding schemes do have analogues in coordination chemistry, and even on metal surfaces in which the internal bonding is highly delocalised, molecular adsorbates appear to form quite local bonds to specific numbers of surface atoms. Carboxylates tend to form bidentate surface bonds through the two O atoms in all the structures investigated in detail so far, although data from vibrational spectroscopies, in particular, suggest that monodentate bonding may occur at different coverages or in different phases. Far more experimental data are required, however, to establish a much wider range of trends in adsorption geometries. Moreover, if structural studies are to be extended to investigations of surface reaction intermediates *under reaction conditions*, very significant developments of methods are probably required.

References

1 K.-M. Schindler, Ph. Hofmann, K.-U. Weiss, R. Dippel, V. Fritzsche, A. M. Bradshaw, D. P. Woodruff, M. E. Davila, M. C. Asensio, J. C. Conesa and A. R. Gonzalez-Elipe, *J. Electron Spectrosc. Relat. Phenom.*, 1993, **64–65**, 75.
2 P. R. Watson, M. A. Van Hove and K. Hermann, *NIST Surface Structure Database Ver. 5.0*, NIST Gaithersburg, MD, 2003.
3 J. B. Pendry, *Low Energy Electron Diffraction*, Academic Press, New York, 1974.
4 M. A. Van Hove, W. H. Weinberg and C.-M. Chan, *Low-energy electron diffraction: experiment, theory and surface structure*, Springer, Berlin, 1986.
5 K. Heinz, *Rep. Prog. Phys.*, 1995, **58**, 637.
6 D. P. Woodruff and A. M. Bradshaw, *Rep. Prog. Phys.*, 1994, **57**, 1029.
7 D. P. Woodruff, *Surf. Sci. Rep.*, 2007, **62**, 1.
8 J. Stöhr, in *X-Ray Absorption, Principles, Techniques, Applications of EXAFS, SEXAFS and XANES*, ed. R. Prins and D. C. Koningsberger, Wiley, New York, 1988, p. 443.
9 D. P. Woodruff, *Rep. Prog. Phys.*, 1986, **49**, 683.
10 J. Stöhr, *NEXAFS Spectroscopy*, Springer-Verlag, Berlin, 1977.
11 J. Stöhr, J. L. Gland, W. Eberhardt, D. Outka, R. J. Madix, F. Sette, R. J. Koestner and U. Doebler, *Phys. Rev. Lett.*, 1983, **51**, 2414.
12 H. Öström, H. Ogasawara, L. Å. Näslund, L. G. M. Pettersson and A. Nilsson, *Phys. Rev. Lett.*, 2006, **96**, 146104.
13 R. Burch, *Phys. Chem. Chem. Phys.*, 2006, **8**, 5483.
14 J. Stöhr, D. Outka, R. J. Madix and U. Döbler, *Phys. Rev. Lett.*, 1985, **54**, 1256.
15 D. Outka, R. J. Madix and J. Stöhr, *Surf. Sci.*, 1985, **164**, 235.
16 A. Puschmann, J. Haase, M. D. Crapper, C. E. Riley and D. P. Woodruff, *Phys. Rev. Lett.*, 1985, **54**, 2250.
17 M. D. Crapper, C. E. Riley, D. P. Woodruff, A. Puschmann and J. Haase, *Surf. Sci.*, 1986, **171**, 1.
18 D. P. Woodruff, C. F. McConville, A. L. D. Kilcoyne, Th. Lindner, J. Somers, M. Surman, G. Paolucci and A. M. Bradshaw, *Surf. Sci.*, 1988, **201**, 228.
19 D. B. W. Yawney and R. J. Doedens, *Inorg. Chem.*, 1970, **9**, 1626.
20 H. Uekusa, S. Ohba, Y. Saito, M. Kato, T. Tokii and Y. Muto, *Acta Crystallogr., Sect. C: Cryst. Struct. Commun.*, 1989, **45**, 377.
21 M. Yamanaka, H. Uekusa, S. Ohba, Y. Saito, S. Iwata, M. Kato, T. Tokaii, Y. Muto and O. W. Seward, *Acta Crystallogr., Sect. B: Struct. Sci.*, 1991, **47**, 344.

22 F. Sapína, M. Burgos, E. Escrivá, J.-V. Folgado, D. Betrán and P. Gómez-Pomero, *Inorg. Chim. Acta*, 1994, **216**, 185.
23 A. Wander and B. W. Holland, *Surf. Sci.*, 1988, **199**, L403.
24 A. Sotiropoulos, P. K. Milligan, B. C. C. Cowie and M. Kadodwala, *Surf. Sci.*, 2000, **444**, 52.
25 Ph. Hofmann, K.-M. Schindler, S. Bao, V. Fritzsche, D. E. Ricken, A. M. Bradshaw and D. P. Woodruff, *Surf. Sci.*, 1994, **304**, 74.
26 S. M. Johnston, A. Mulligan, V. Dhanak and M. Kadodwala, *Surf. Sci.*, 2003, **530**, 111.
27 Th. Lindner, J. Somers, A. M. Bradshaw, A. L. D. Kilcoyne and D. P. Woodruff, *Surf. Sci.*, 1988, **203**, 333.
28 D. A. Outka, R. J. Madix and J. Stöhr, *Surf. Sci.*, 1985, **164**, 235.
29 M. Bader, A. Puschmann and J. Haase, *Phys. Rev. B: Condens. Matter Mater. Phys.*, 1986, **33**, 7336.
30 E. Holub-Krappe, K. C. Prince, K. Horn and D. P. Woodruff, *Surf. Sci.*, 1986, **173**, 176.
31 S. A. Chambers, S. Thevuthasan, Y. J. Kim, G. S. Herman, Z. Wang, E. D. Tober, R. X. Ynzunza, J. Morais, C. H. F. Peden, K. Ferris and C. S. Fadley, *Chem. Phys. Lett.*, 1997, **267**, 51.
32 S. Thevuthasan, G. S. Herman, Y. J. Kim, S. A. Chambers, C. H. F. Peden, Z. Wang, R. X. Ynzunza, E. D. Tober, J. Morais and C. S. Fadley, *Surf. Sci.*, 1998, **401**, 261.
33 D. I. Sayago, M. Polcik, R. Lindsay, J. T. Hoeft, M. Kittel, R. L. Toomes and D. P. Woodruff, *J. Phys. Chem. B*, 2004, **108**, 14316.
34 A. Gutiérrez-Sosa, P. Martínez-Escolano, H. Raza, R. Lindsay, P. L. Wincott and G. Thornton, *Surf. Sci.*, 2001, **471**, 163.
35 B. E. Hayden, A. King and M. A. Newton, *J. Phys. Chem. B*, 1999, **103**, 203.
36 P. Käckell and K. Terakura, *Surf. Sci.*, 2000, **461**, 191.
37 E. A. Kröger, D. I. Sayago, F. Allegretti, M. J. Knight, M. Polcik, W. Unterberger, T. J. Lerotholi, K. A. Hogan, C. L. A. Lamont, M. Cavalleri, K. Hermann and D. P. Woodruff, *Surf. Sci.*, 2008, **602**, 1267.
38 K.-U. Weiss, R. Dippel, K.-M. Schindler, P. Gardner, V. Fritzsche, A. M. Bradshaw, A. L. D. Kilcoyne and D. P. Woodruff, *Phys. Rev. Lett.*, 1992, **69**, 3196.
39 S. M. Johnston, G. Rousseau, V. Dhanak and M. Kadodwala, *Surf. Sci.*, 2001, **477**, 163.
40 M. Pascal, C. L. A. Lamont, M. Kittel, J. T. Hoeft, R. Terborg, M. Polcik, J. H. Kang, R. Toomes and D. P. Woodruff, *Surf. Sci.*, 2001, **492**, 285.
41 F. Schreiber, *Prog. Surf. Sci.*, 2000, **65**, 151.
42 A. Ulman, *Chem. Rev.*, 1996, **96**, 1533.
43 D. P. Woodruff, *Appl. Surf. Sci.*, 2007, **254**, 76.
44 N. A. Booth, D. P. Woodruff, O. Schaff, T. Gießel, R. Lindsay, P. Baumgartel and A. M. Bradshaw, *Surf. Sci.*, 1998, **397**, 258.
45 J.-H. Kang, R. L. Toomes, M. Polcik, M. Kittel, J.-T. Hoeft, V. Efstathiou, D. P. Woodruff and A. M. Bradshaw, *J. Chem. Phys.*, 2003, **118**, 6059.
46 D. I. Sayago, M. Polcik, G. Nisbet, C. L. A. Lamont and D. P. Woodruff, *Surf. Sci.*, 2005, **590**, 76.
47 O. Schaff, G. Hess, V. Fritzsche, V. Fernandez, K.-M. Schindler, A. Theobald, Ph. Hofmann, A. M. Bradshaw, R. Davis and D. P. Woodruff, *Surf. Sci.*, 1995, **331–333**, 201.
48 M. Kerkar, A. B. Hayden, D. P. Woodruff, M. Kadodwala and R. G. Jones, *J. Phys.: Condens. Matter*, 1992, **4**, 5043.
49 A. F. Carley, P. R. Davies and G. G. Mariotti, *Surf. Sci.*, 1998, **401**, 400.
50 M. Kittel, D. I. Sayago, J. T. Hoeft, M. Polcik, M. Pascal, C. L. A. Lamont, R. L. Toomes and D. P. Woodruff, *Surf. Sci.*, 2002, **516**, 237.
51 X.-C. Guo and R. J. Madix, *Surf. Sci.*, 2001, **489**, 37.
52 X.-C. Guo and R. J. Madix, *J. Phys. Chem. B*, 2001, **105**, 3878.
53 J. Robinson and D. P. Woodruff, *Surf. Sci.*, 2004, **556**, 193.
54 R. J. Madix, J. L. Solomon and J. Stöhr, *Surf. Sci.*, 1998, **197**, L253.
55 M. Bader, B. Hillert, A. Puschmann, J. Haase and A. M. Bradshaw, *Europhys. Lett.*, 1988, **5**, 443.
56 J. E. Demuth and D. E. Eastman, *Phys. Rev. Lett.*, 1974, **32**, 1123.
57 S. Lehwald and H. Ibach, *Surf. Sci.*, 1979, **89**, 425.
58 S. Bao, Ph. Hofmann, K.-M. Schindler, V. Fritzsche, A. M. Bradshaw, D. P. Woodruff, C. Casado and M. C. Asensio, *Surf. Sci.*, 1994, **307–309**, 722.
59 S. Bao, Ph. Hofmann, K.-M. Schindler, V. Fritzsche, A. M. Bradshaw, D. P. Woodruff, C. Casado and M. C. Asensio, *Surf. Sci.*, 1995, **323**, 19.
60 L. L. Kesmodel, L. H. Dubois and G. A. Somorjai, *J. Chem. Phys.*, 1979, **70**, 2180.
61 U. Starke, A. Barbieri, N. Materer, M. A. Van Hove and G. A. Somorjai, *Surf. Sci.*, 1993, **286**, 1.
62 R. J. Koestner, M. A. Van Hove and G. A. Somorjai, *Surf. Sci.*, 1982, **121**, 321.
63 A. Wander, M. A. Van Hove and G. A. Somorjai, *Phys. Rev. Lett.*, 1991, **67**, 626.
64 A. Barbieri, M. A. Van Hove and G. A. Somorjai, in *The Structure of Surfaces IV*, ed. X. D. Xie, S. Y. Tong and M. A. Van Hove, World Scientific, Singapore, 1994, p. 201.
65 G. S. Blackman, C. T. Kao, B. E. Bent, C. M. Mate, M. A. Van Hove and G. A. Somorjai, *Surf. Sci.*, 1988, **207**, 66.
66 M. J. Knight, F. Allegretti, E. A. Kröger, M. Polcik, C. L. A. Lamont and D. P. Woodruff, *Surf. Sci.*, DOI: 10.1016/j.susc.2008.06.038.
67 R. M. Ormerod, C. J. Baddeley, C. Hardacre and R. M. Lambert, *Surf. Sci.*, 1996, **360**, 1.
68 T. E. Caldwell, I. M. Abdelrehim and D. P. Land, *J. Am. Chem. Soc.*, 1996, **118**, 907.
69 T. E. Caldwell and D. P. Land, *J. Phys. Chem. B*, 1999, **103**, 7869.
70 M. R. Churchill, L. A. Buttrey, J. B. Keister, J. W. Ziller, T. S. Janik and W. S. Striejewske, *Organometallics*, 1990, **9**, 766.
71 H. Dietrich, K. Jacobi and G. Ertl, *J. Chem. Phys.*, 1997, **106**, 9313.
72 B. Afsin, P. R. Davies, A. Pushusky and M. W. Roberts, *Surf. Sci.*, 1991, **259**, L724.
73 B. Afsin, P. R. Davies, A. Pushusky, M. W. Roberts and D. Vincent, *Surf. Sci.*, 1993, **284**, 109.
74 C. J. Hirschmugl, K.-M. Schindler, O. Schaff, V. Fernandez, A. Theobald, Ph. Hofmann, A. M. Bradshaw, R. Davis, N. A. Booth, D. P. Woodruff and V. Fritzsche, *Surf. Sci.*, 1996, **352–354**, 232.
75 P. Baumgärtel, R. Lindsay, T. Giessel, O. Schaff, A. M. Bradshaw and D. P. Woodruff, *J. Phys. Chem. B*, 2000, **104**, 3044.
76 K.-M. Schindler, V. Fritzsche, M. C. Asensio, P. Gardner, D. E. Ricken, A. W. Robinson, A. M. Bradshaw, D. P. Woodruff, J. C. Conesa and A. R. Gonzalez-Elipe, *Phys. Rev. B: Condens. Matter Mater. Phys.*, 1992, **46**, 4836.
77 Y. Zheng, E. Moler, E. Hudson, Z. Hussain and D. A. Shirley, *Phys. Rev. B: Condens. Matter Mater. Phys.*, 1993, **48**, 4760.
78 N. A. Booth, R. Davis, R. Toomes, D. P. Woodruff, C. Hirschmugl, K.-M. Schindler, O. Schaff, V. Fernandez, A. Theobald, Ph. Hofmann, R. Lindsay, T. Gießel, P. Baumgärtel and A. M. Bradshaw, *Surf. Sci.*, 1997, **387**, 152.
79 N. Franco, J. Avila, M. E. Davila, M. C. Asensio, D. P. Woodruff, O. Schaff, V. Fernandez, K.-M. Schindler, V. Fritzsche and A. M. Bradshaw, *Phys. Rev. Lett.*, 1997, **79**, 673.
80 N. Franco, J. Avila, M. E. Davila, M. C. Asensio, D. P. Woodruff, O. Schaff, V. Fernandez, K.-M. Schindler, V. Fritzsche and A. M. Bradshaw, *J. Phys.: Condens. Matter*, 1997, **9**, 8419.
81 K. Takayanagi, Y. Tanishiro, M. Takahashi and S. Takahashi, *J. Vac. Sci. Technol., A*, 1985, **3**, 1502.
82 M. L. Colaianni, P. J. Chen and J. T. Yates, *J. Chem. Phys.*, 1992, **96**, 7826.
83 P. J. Chen, M. L. Colaianni and J. T. Yates, *Surf. Sci.*, 1992, **274**, L605.
84 M. Bjrkqvist, M. Gthelid, T. M. Grehk and U. O. Karlsson, *Phys. Rev. B: Condens. Matter Mater. Phys.*, 1998, **57**, 2327.
85 S. Bengió, H. Ascolani, N. Franco, J. Avila, M. C. Asensio, A. M. Bradshaw and D. P. Woodruff, *Phys. Rev. B: Condens. Matter Mater. Phys.*, 2004, **69**, 125340.
86 P. Jakob, *Chem. Phys. Lett.*, 1996, **263**, 607.
87 D. R. Mullins, Lj. Kundakovic and S. H. Overbury, *J. Catal.*, 2000, **195**, 169.
88 J. H. Miners, A. M. Bradshaw and P. Gardner, *Phys. Chem. Chem. Phys.*, 1999, **1**, 4909.
89 F. Huerta, E. Morallón, F. Cases, A. Rodes, J. L. Vázquez and A. Aldaz, *J. Electroanal. Chem.*, 1997, **431**, 269.
90 R. E. Benner, K. U. von Raben, R. Dornhaus, R. K. Chang, B. L. Laube and F. A. Otter, *Surf. Sci.*, 1981, **102**, 7.

91 K. Kunimatsu, H. Seki, W. G. Golden, J. G. Gordon II and M. R. Philpott, *Surf. Sci.*, 1985, **158**, 596.
92 D. S. Corrigan, P. Gao, L.-W. H. Leung and M. J. Weaver, *Langmuir*, 1986, **2**, 744.
93 W. Daum, F. Dederichs and J. E. Müller, *Phys. Rev. Lett.*, 1998, **80**, 766; (erratum), *Phys. Rev. Lett.*, 2000, **85**, 2655.
94 N. A. Booth, R. Davis, D. P. Woodruff, D. Crysostomou, T. McCabe, D. R. Lloyd, O. Schaff, V. Fernandez, S. Bao, K.-M. Schindler, R. Lindsay, J. T. Hoeft, R. Terborg, P. Baumgartel and A. M. Bradshaw, *Surf. Sci.*, 1998, **416**, 448.
95 D. Brown, D. P. Woodruff, T. C. Q. Noakes and P. Bailey, *Surf. Sci.*, 2001, **476**, L241.
96 C. Bittencourt, E. A. Soares and D. P. Woodruff, *Surf. Sci.*, 2003, **526**, 33.
97 F. Bondino, A. Baraldi, H. Over, G. Comelli, P. Lacovig, S. Lizzit, G. Paolucci and R. Rosei, *Phys. Rev. B: Condens. Matter Mater. Phys.*, 2001, **64**, 085422.
98 F. Bondino, E. Vesselli, A. Baraldi, G. Comelli, A. Verdini, A. Cossaro, L. Floreano and A. Morgante, *J. Chem. Phys.*, 2003, **118**, 10735.
99 K. Besenthal, G. Chiarello, M. E. Kordesch and H. Conrad, *Surf. Sci.*, 1986, **178**, 667.
100 M. E. Kordesch, W. Stenzel and H. Conrad, *Surf. Sci.*, 1987, **186**, 601.
101 W. H. Wienberg, D. F. Johnson, Y.-Q. Wang, J. E. Parmeter and M. M. Hills, *Surf. Sci.*, 1990, **235**, L299.
102 M. E. Kordesch, W. Feng, W. Stenzel, M. Weaver and H. Conrad, *J. Electron Spectrosc. Relat. Phenom.*, 1987, **44**, 149.
103 M. J. Harrison, D. P. Woodruff and J. Robinson, *Surf. Sci.*, 2006, **600**, 340.
104 J. Haase, *J. Phys.: Condens. Matter*, 1997, **9**, 3647.
105 T. Nakahashi, S. Terada, T. Yokoyama, H. Hamamatsu, Y. Kitajima, M. Sakano, F. Matsui and T. Ohta, *Surf. Sci.*, 1997, **373**, 1.
106 G. J. Jackson, S. M. Driver, D. P. Woodruff, N. Abrams, R. G. Jones, M. Butterfield, M. D. Crapper, B. C. C. Cowie and V. Formoso, *Surf. Sci.*, 2000, **459**, 231.
107 G. J. Jackson, D. P. Woodruff, A. S. Y. Chan, R. G. Jones and B. C. C. Cowie, *Surf. Sci.*, 2005, **577**, 31.
108 M. J. Harrison, D. P. Woodruff and J. Robinson, *Surf. Sci.*, 2006, **600**, 1827.